



## Effect of partitioning time on microstructural evolution of C-Mn-Si steel in one-step quenching and partitioning process

H.R. Ghazvinloo\*, A. Honarbakhsh-Raouf

Department of Materials Engineering, Semnan University, Semnan, Iran.

Received 30 June 2014; Revised 25 July 2014; Accepted 25 July 2014.

\*Corresponding Author. E-mail: [Hamid.Ghazvinloo@gmail.com](mailto:Hamid.Ghazvinloo@gmail.com); Tel: (+982333484586)

### Abstract

Quenching and partitioning process focuses on carbon enrichment of austenite phase during a partitioning treatment after initial quenching below the martensite start temperature ( $M_s$ ). In one-step quenching and partitioning process, steel is partitioned at same quenching temperature whereas in the two-step quenching and partitioning process, the partitioning treatment performs at a temperature above the quenching temperature. Austenitizing conditions, quenching temperature, partitioning time and temperature are the important parameters for this heat treatment. The effect of partitioning time on microstructural evolution in a C-Mn-Si steel during one-step quenching and partitioning process was investigated in present work. For this aim, after full austenitization at 900 °C, specimens were quenched into an oil bath at 238 °C then partitioned at this temperature for 10, 30, 100, 700 and 1000 s, finally water quenched to room temperature. Having finished the heat treatments, the resulted multiphase microstructures were evaluated by optical microscopy and scanning electron microscopy; then, the retained austenite volume fraction and its average carbon content were measured by X-ray diffraction method in the heat treated specimens.

**Keywords:** One-step quenching and partitioning, partitioning time, microstructure, retained austenite.

### 1. Introduction

The development of steels containing combinations of martensite and austenite is one of the most promising approaches being explored for the creation of new advanced high-strength steels (AHSS) [1]. A process referred to as quenching and partitioning (Q&P) was introduced by Speer et al. [2] in 2003 to create steel microstructures that contain martensite/austenite mixtures with tailored mechanical properties [3-7]. Q&P process can lead to a multiphase structure with hard matrix and retained austenite which the initial and fresh martensites can provide a high tensile strength while the retained austenite can provide a good ductility, and the obtained multiphase microstructure can prohibit crack initiation and propagation effectively [8]. The Q&P process includes: [9-12] (1) a partial or full austenitizing heat treatment, (2) fast quenching to a temperature below the martensite start temperature ( $M_s$ ) but above the martensite finish temperature ( $M_f$ ), to produce a controlled volume fraction of supersaturated martensite and untransformed austenite, (3) subsequent partitioning during quenching (one-step treatment) or above the  $M_s$  temperature (two-step treatment), to produce the complete diffusion of carbon from martensite to residual austenite (carbide precipitation is prevented by alloying with Si or Al), and (4) quenching to room temperature. Consequently, the final microstructure contains ferrite (in the case of partial austenitization), martensite and retained austenite.

A more accurate description of the microstructure is essential for better understanding of the microstructure formation and better control of the final properties of the material [13]. Therefore, the goal of the present work is to investigate the effect of partitioning time as an important parameter on microstructural evolution in a C-Mn-Si steel during one-step quenching and partitioning process.

### 2. Materials and methods

#### 2.1. Materials

The chemical composition of the investigated material in this study has been shown in Table 1. 1.24 wt.% manganese was included in the chemical composition to retard ferrite, pearlite and bainite formation and to decrease the bainite start

temperature, as well as to enhance the austenite stability and a silicon content of 1.38 wt.% was used to restrict carbide precipitation during the partitioning step [14].

**Table 1:** The chemical composition of the investigated material (wt.%).

C	0.362	Mo	0.005
Si	1.38	Ni	0.0902
Mn	1.24	Al	0.03
P	0.0245	Co	0.0101
S	0.0202	Cu	0.0711
Cr	0.0973	B	0.002
Nb	0.0025	Ca	0.0008
Ti	0.0023	Zr	0.002
V	0.002	As	0.0101
W	0.015	Sn	0.0095
Pb	0.025	Fe	Base

### 2.2. One-step Q&P heat treatment

For one-step Q&P heat treatment, the specimens were heated to 900 °C at heating rate of +5 °C/s in a furnace and held for 10 minutes for full austenitization, then quenched into an oil bath at 238 °C (optimum quenching temperature) with cooling rate of -220 °C/s. In continue, they were partitioned at this temperature for 10, 30, 100, 700 and 1000 s, respectively, finally water quenched to room temperature (Figure 1).

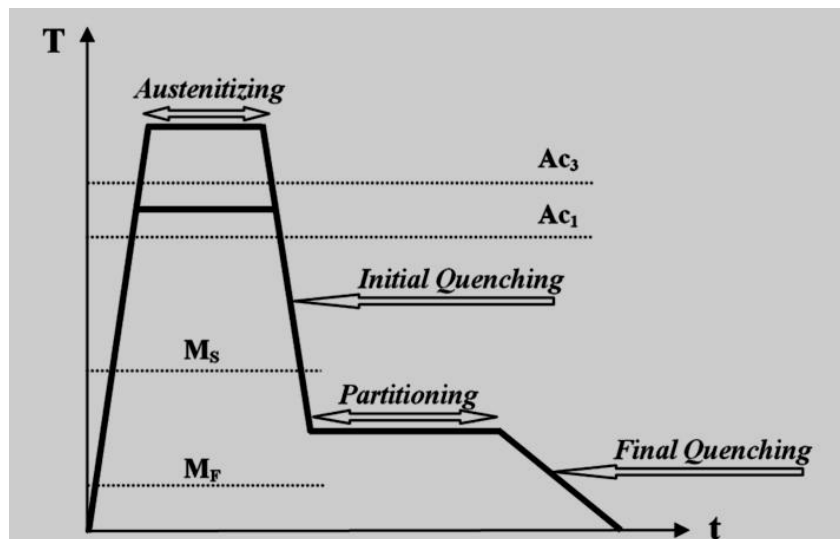


**Figure 1:** Schematic of one-step Q&P process applied in present work ( $M_s=339$  °C,  $Ac_1=748.1$  °C,  $Ac_3=841.5$  °C).

### 2.3. Characterization

Having finished the heat treatments, the treated samples were ground and polished mechanically then etched with 2% nital for 6-8 s. After conventional metallographic preparation, the microstructural examination of the samples was conducted using optical microscopy and JEOL JXA-840 scanning electron microscopy (SEM). In order to determine the retained austenite volume fraction and its average carbon content in the specimens treated by one-step Q&P process, X-ray diffraction (XRD) measurements were performed on a Bruker D8 diffractometer using  $CuK\alpha$  radiation operating at 35 kV and 30 mA. Samples were scanned over a  $2\theta$  range from 10 to 90 deg with a dwelling time of 1s and a step size of 0.05 deg. The volume fraction of retained austenite was measured based on the direct comparison method [15] by using the integrated intensity of the  $(200)_\gamma$ ,  $(220)_\gamma$ ;  $(200)_M$ ,  $(211)_M$  peaks and the average carbon content of retained austenite was measured according to following equation [16]. The average carbon content obtained from both austenite peak positions was calculated [17] in this study.

$$a_0 = 3.555 + 0.044x$$

Where  $a_0$  is austenite lattice parameter in angstroms and  $x$  is average carbon content of austenite in weight percent.

### 3. Results and discussion

#### 3.1. Optical microscopy observations

Optical micrographs showing the morphology of the specimens treated by one-step Q&P process with partitioning times of 10, 100, and 1000 s have been shown in Figure 2. According to it, a mixture of martensite and carbon-enriched retained austenite phases was separably observed in the all specimens partitioned in different times.

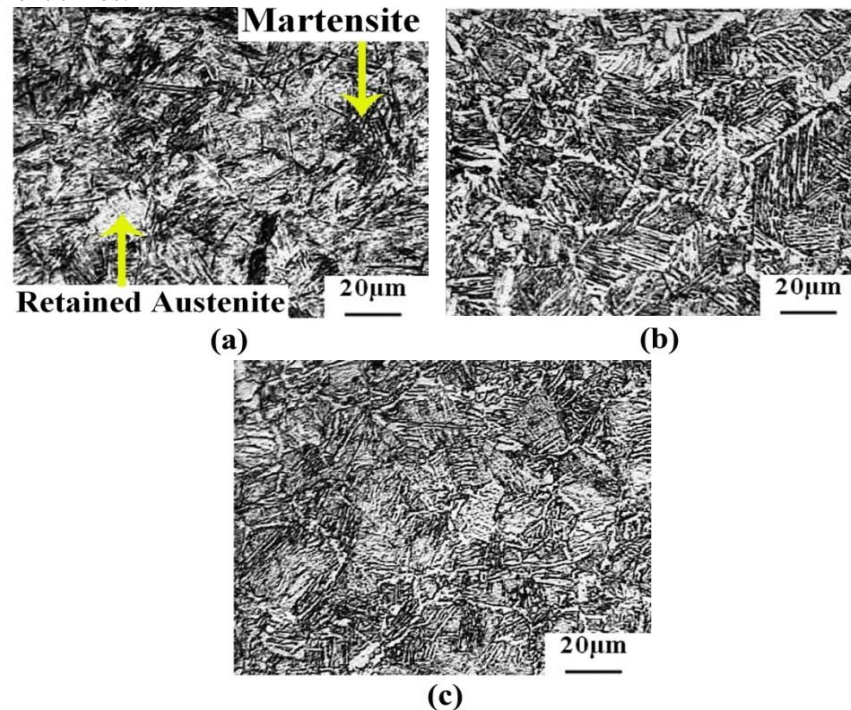


**Figure 2:** optical micrographs for heat treated specimens: full austenitized at 900 °C, quenched to 238 °C, partitioned at 238 °C for (a)10 (b)100 and (c)1000 s and finally water quenched to room temperature.

Base on Koistinen–Marburger relationship (following equation) [18], the volume fraction of virgin martensite and untransformed austenite after quenching at 238 °C and prior to partitioning process were approximately predicted 67 and 33 vol pct.

$$f_m = 1 - e^{-0.011(M_s - QT)}$$

Where  $M_s$  is martensite start temperature,  $QT$  is quenching temperature and  $f_m$  is the fraction of martensite produced in quenching temperature ( $QT$ ).

Since, the carbon content of steel used in this study was less than 0.6 wt.%; hence, the virgin martensite has had a lath morphology. After the second quenching to room temperature, a proportion of untransformed austenite with enough carbon content could be stabilized at room temperature, another proportion of untransformed austenite with a carbon content enough high transformed into twin martensite and the rest of the untransformed austenite with a lower carbon content transformed into plate or lath martensite at room temperature [19]. Optical microscopy observations give indications about the microstructure present in the specimens for every Q&P condition. However, they do not provide microstructural details smaller than a few microns [20]; therefore, SEM was used for these purposes.

#### 3.2. SEM observations

The SEM micrographs for heat treated specimens have been shown in Figure 3. According to it, two kinds of retained austenite with different morphology and size were existed in specimens. One was the island-like shape and distributed along the grain boundary mainly, and a few of them distributed within martensite matrix; the other was the film-like shape and distributed between martensite laths [21]. Cementite carbide ( $Fe_3C$ ) precipitation was observed in specimens partitioned for longer partitioning times such as 700 and 1000 s.

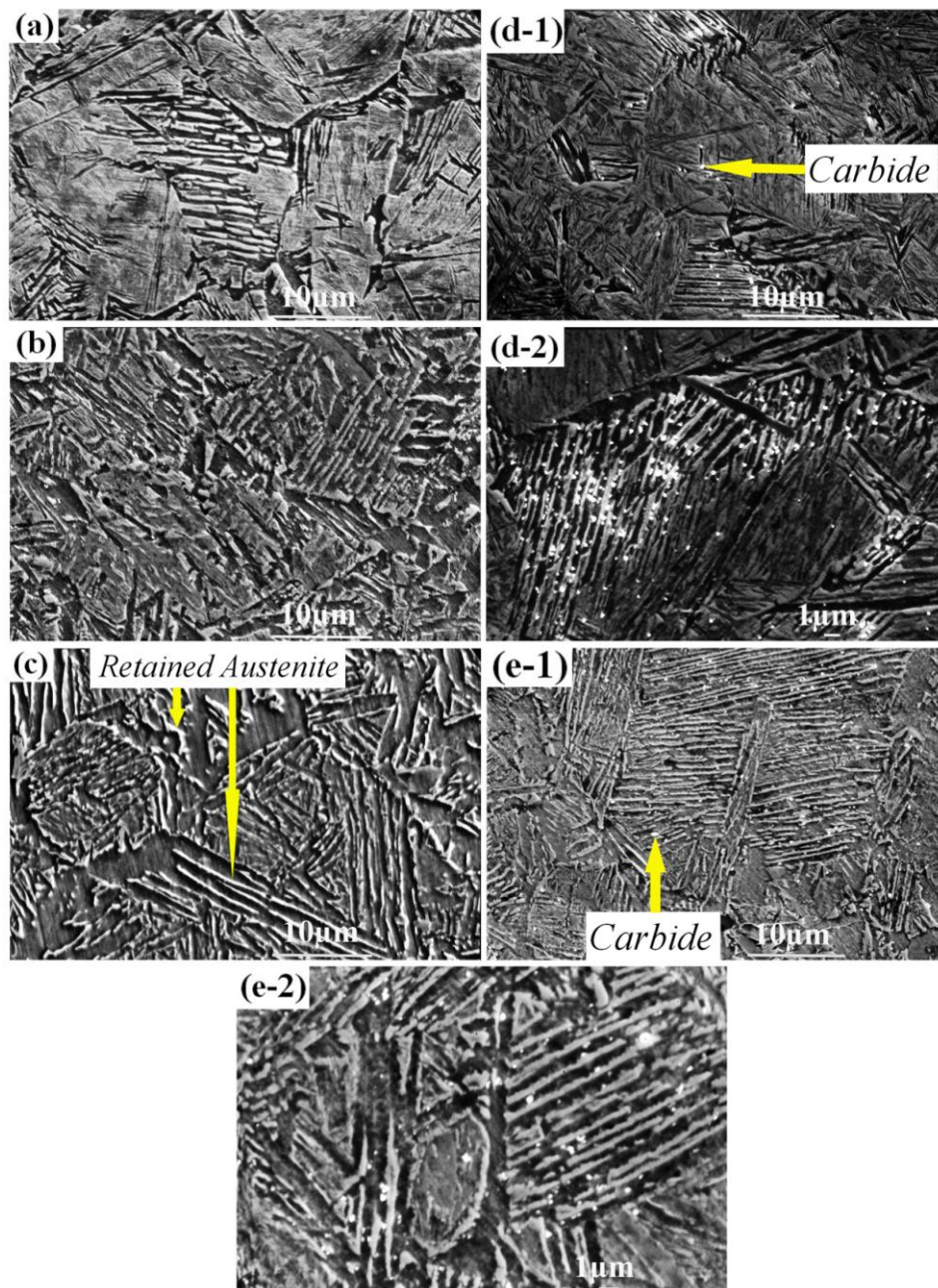


**Figure 3:** SEM micrographs of the treated specimens: full austenitized at 900 °C, quenched to 238 °C, partitioned at 238 °C for (a)10 (b)30 (c)100 (d)700 (e)1000 s, and finally water quenched to room temperature.

### 3.3. XRD Analysis

The average carbon content obtained in different partitioning times has been shown in Figure 4. The highest average carbon content was 1.5205% which obtained at partitioning time of 10 s and it may be due to the rapid partitioning kinetics and high potential of carbon partitioning from supersaturated martensite to untransformed austenite at primal times of partitioning process. The average carbon content of retained austenite decreased intensively to 1.2886% in specimen partitioned for 30 s. It can be due to processes related with the conventional martensite tempering, like carbon segregation in martensite. It can reduce the amount of carbon available for the enrichment of the austenite during the partitioning step [13]. The diffusion of more carbon atoms from supersaturated martensite to untransformed austenite during longer partitioning times (100 s) resulted in an increasing in average carbon content of retained austenite to 1.4022%. Carbide precipitation decreases average carbon content of retained austenite because carbide formation consumes certain amount of carbon in martensite, therefore there may not be enough carbon for the stabilization of untransformed austenite during cooling from partitioning temperature to room temperature [22]. But apparently, the kinetics

of carbon partitioning has been a dominant process especially at 700 s of partitioning time as it has led to an increasing in the average carbon content to 1.4318% and restrained from severe decreasing in average carbon content of retained austenite at partitioning time of 1000 s.

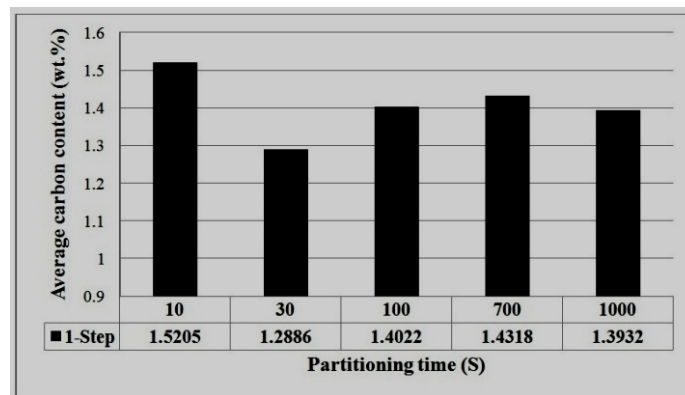


**Figure 4:** The average carbon content of retained austenite measured for different partitioning times.

Retained austenite plays the key role on plasticity enhancement. As been pointed out in Ref. [23], interlath film-like austenite can impede generation and propagation of cracks and in turn improve toughness effectively; Furthermore, both interlath and island-like austenite can partially transform to martensite and show ‘TRIP’ effect during deformation, eliminating stress concentration and retarding the happening of necking [24], which results in the increasing of both strength and elongation. The retained austenite volume fraction measured in different partitioning times has been shown in Figure 5. Also, XRD patterns of steel treated by Q&P process with the maximum and minimum volume fraction of retained austenite have been shown in Figure 6. The maximum volume fraction of retained austenite in this study was 11.83% which obtained at partitioning time of 10 s and it was due to high average carbon content of untransformed austenite in this condition but it decreased intensively to 7.23% in specimen partitioned for 30 s because of severe decreasing in average carbon content of untransformed austenite in this state. Increasing in average carbon content of untransformed austenite to 1.4022, 1.4318 and 1.3932% at partitioning time of 100, 700 and 1000 s resulted in increasing in retained austenite volume fraction to 10.85, 10.43 and 10.73%, respectively. With increasing in average carbon content of untransformed austenite during partitioning stage, its  $M_s$  temperature decreases and its thermal stability increases. Therefore, carbon enrichment of untransformed austenite by partitioning process can increase the volume fraction of retained austenite.

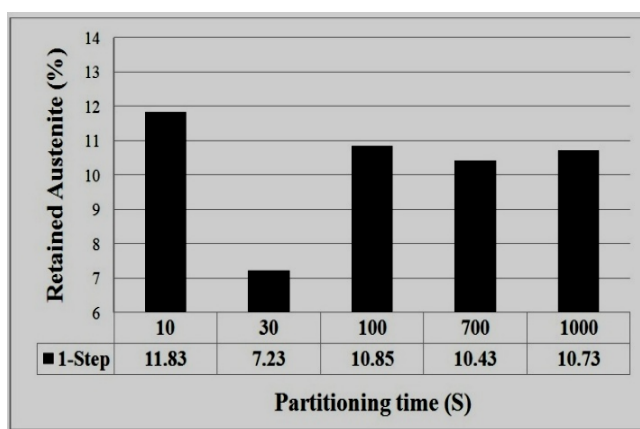


**Figure 5:** The retained austenite volume fraction measured for different partitioning times.

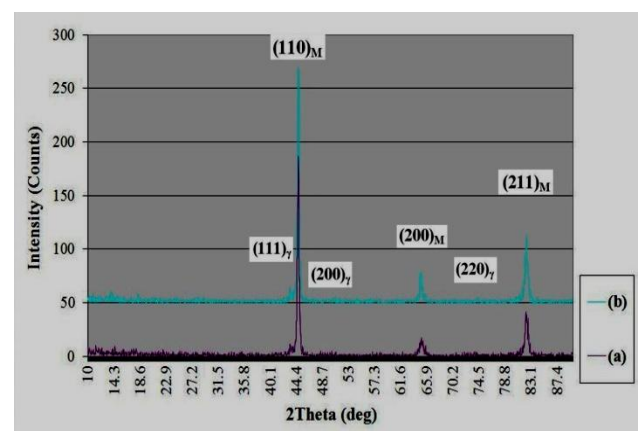


**Figure 6:** XRD patterns of steel treated by one-step Q&P process with the (a) maximum and (b) minimum volume fraction of retained austenite.

## Conclusion

The behaviour of a C-Mn-Si steel under the one-step Q&P process was studied whereas under the two-step Q&P process had been studied in previous literature [25]. In this study, two kinds of retained austenite with different morphology and size were observable. One was the island-like shape and distributed along the grain boundary mainly, and a few of them distributed within martensite matrix; the other was the film-like shape and distributed between martensite laths. Also, Carbide precipitation occurrence was observed in specimens partitioned at 238 °C for longer partitioning times (700 and 1000 s). With increasing in average carbon content of untransformed austenite during partitioning stage, its  $M_s$  temperature decreases and its thermal stability increases. Therefore, carbon enrichment of untransformed austenite with partitioning process will increase the volume fraction of retained austenite. The highest average carbon content in this study was 1.5205% which obtained at partitioning time of 10 s. Also, the greatest retained austenite volume fraction was 11.83% which obtained at partitioning time of 10 s and it was due to high average carbon content of untransformed austenite in this condition.

## Acknowledgements

The authors would like to thank of Dr. Ali Reza Kiani Rashid for his assistance in the preparation of this article, and Oghabafshan Industrial & Manufacturing Company and Semnan University for all the facilities.

## References

1. Matlock D. K., Speer J. G. *Microstructure and texture in steels*, 185 (2009).
2. Speer J. G., Streicher A. M., Matlock D. K., Rizzo, F. C., Krauss G. Austenite formation and decomposition, (2003) Warrendale, PA:TMS/ISS.
3. Speer J. G., Edmonds D. V., Rizzo F. C., Matlock D. K. *Curr. Opin. Solid State Mater. Sci.* 8 (2004) 219.
4. De Moor E., Lacroix S., Clarke A. J., Penning J., Speer J. G. *Metall. Mater. Trans. A.* 39A (2008) 2586.
5. De Moor E., Föjler C., Clarke A. J., Penning J., Speer J. G. (2008) TMS, Warrendale, PA.
6. Clarke A. J. Ph.D. Thesis, Colorado School of Mines, Golden, CO (2006).
7. Streicher A. M., Speer J. G., Matlock D. K., De Cooman B. C. (2004) Warrendale, PA: AIST.
8. Wang C. Y., Shi J., Cao W. Q., Dong H. *Mater. Sci. Eng. A.* 527 (2010) 3442.
9. Clarke A. J., Speer J. G., Miller M. K., Hackenberg R. E., Edmonds D. V., Matlock D. K., Rizzo F. C., Clarke K. D., De Moor E. *Acta Mater.* 56 (2008) 16.
10. Kim D. H., Speer J. G., Kim H. S., De Cooman B. C. *Metall. Mater. Trans. A.* 40 (2009) 2048.
11. Santofimia M. J., Speer J. G., Clarke A. J., Zhao L., Sietsma J. *Acta Mater.* 57 (2009) 4548.
12. De Moor E., Lacroix S., Clarke A. J., Penning J., Speer J. G. *Metall. Mater. Trans. A.* 39 (2008) 2586.
13. Santofimia M. J., Zhao L., Petrov R., Sietsma J. *Mater. Charac.* 59 (2008) 1758.
14. Santofimia M. J., Zhao L., Petrov R., Kwakernaak C., Sloof W. G., Sietsma J. *Acta Mater.* 59 (2011) 6059.
15. Cullity B. D., Stock S. R. *Elements of X-ray Diffraction*, 3rd ed., Prentice Hall, New York (2001).
16. Cullity B. B. *Elements of X-Ray Diffraction*, 2nd ed., Addison-Wesley Publishing Co., Inc. (1978).
17. De Moor E., Lacroix S., Clarke A. J., Penning J., Speer J. G. *Metall. Mater. Trans. A.* 39A (2008) 2586.
18. Krauss G., *STEELS: Heat treatment and processing principles*; ASM International, Second Edition (1990).
19. Li H. Y., Lu X. W., Li W. J., Jin X. J. *Metall. Mater. Trans. A.* 41A (2010) 1284.
20. Santofimia M. J., Zhao L., Sietsma J. *Metall. Mater. Trans. A.* 40A (2009) 46.
21. Wang X. D., Guo Z. H., Rong Y. H. *Mater. Sci. Eng. A.* 529 (2011) 35.
22. Zhong N., Wang X. D., Wang L., Rong Y. H. *Mater. Sci. Eng. A.* 506 (2009) 111.
23. Rao B.V.N, Thomas G. *Metall. Trans.* 11A (1980) 441.
24. Wang X. D., Huang B. X, Rong Y. H., Wang L. *J. Mater. Sci. Technol.* 22 (2006) 625.
25. Ghazvinloo H. R., Honarbakhsh-Raouf A. *J. Mater. Environ. Sci.* 5 (2014) 1988.

(2015) ; <http://www.jmaterenvironsci.com>